

## Percolation of partially interdependent scale-free networks

Di Zhou,<sup>1</sup> Jianxi Gao,<sup>1,2</sup> H. Eugene Stanley,<sup>1</sup> and Shlomo Havlin<sup>3</sup>

<sup>1</sup>*Center for Polymer Studies and Department of Physics, Boston University, Boston, Massachusetts 02215, USA*

<sup>2</sup>*Department of Automation, Shanghai Jiao Tong University, 800 Dongchuan Road, Shanghai 200240, P.R. China*

<sup>3</sup>*Department of Physics, Bar-Ilan University, Ramat-Gan 52900, Israel*

(Received 21 February 2013; published 29 May 2013)

We study the percolation behavior of two interdependent scale-free (SF) networks under random failure of  $1-p$  fraction of nodes. Our results are based on numerical solutions of analytical expressions and simulations. We find that as the coupling strength between the two networks  $q$  reduces from 1 (fully coupled) to 0 (no coupling), there exist two critical coupling strengths  $q_1$  and  $q_2$ , which separate three different regions with different behavior of the giant component as a function of  $p$ . (i) For  $q \geq q_1$ , an abrupt collapse transition occurs at  $p = p_c$ . (ii) For  $q_2 < q < q_1$ , the giant component has a hybrid transition combined of both, abrupt decrease at a certain  $p = p_c^{\text{jump}}$  followed by a smooth decrease to zero for  $p < p_c^{\text{jump}}$  as  $p$  decreases to zero. (iii) For  $q \leq q_2$ , the giant component has a continuous second-order transition (at  $p = p_c$ ). We find that (a) for  $\lambda \leq 3$ ,  $q_1 \equiv 1$ ; and for  $\lambda > 3$ ,  $q_1$  decreases with increasing  $\lambda$ . Here,  $\lambda$  is the scaling exponent of the degree distribution,  $P(k) \propto k^{-\lambda}$ . (b) In the hybrid transition, at the  $q_2 < q < q_1$  region, the mutual giant component  $P_\infty$  jumps discontinuously at  $p = p_c^{\text{jump}}$  to a very small but nonzero value, and when reducing  $p$ ,  $P_\infty$  continuously approaches to 0 at  $p_c = 0$  for  $\lambda < 3$  and at  $p_c > 0$  for  $\lambda > 3$ . Thus, the known theoretical  $p_c = 0$  for a single network with  $\lambda \leq 3$  is expected to be valid also for strictly partial interdependent networks.

DOI: [10.1103/PhysRevE.87.052812](https://doi.org/10.1103/PhysRevE.87.052812)

PACS number(s): 89.75.Hc, 64.60.ah, 89.75.Fb

### I. INTRODUCTION

Complex networks appear in almost every aspect of science and technology [1–15]. An important property of a network is its robustness in terms of node and link failures. The robustness of a network is usually characterized by the value of the critical threshold analyzed by percolation theory. Recently, motivated by the fact that modern infrastructures are significantly coupled together, the robustness of interdependent networks has been studied [16–29]. In interdependent networks, the failure of nodes in one network generally leads to failure of dependent nodes in other networks, which in turn may cause further damage to the first network, leading to cascading failures and catastrophic consequences.

The structure of complex networks is frequently non-homogeneous with a broad degree distribution. In many cases, the degree distribution obeys a power-law form, and the networks are called scale-free (SF) [2]. Real networks that have been found to be well approximated by power-law degree distribution include, among many others, the Internet, airline networks, protein regulatory networks, and research collaboration networks [2,5,6]. Thus, the analysis of interdependent scale-free networks with a power-law degree distribution  $P(k) \propto k^{-\lambda}$  is needed. Buldyrev *et al.* [30] developed a framework, based on percolation theory, to study the robustness of interdependent networks. Analysis of fully interdependent scale-free networks (where all nodes in one network depend on all nodes in the other network and vice versa) shows [30] that the critical threshold is  $p_c > 0$  even for  $\lambda \leq 3$ , in contrast to a single network where  $p_c = 0$  [7]. In general, for fully interdependent networks with the same average degree, the broader the degree distribution is (smaller value of  $\lambda$ ), the larger  $p_c$  is [30]. This means that networks with a broader degree distribution become less robust compared to networks with a narrower degree distribution. This feature is in contrast to the trend known in single noninteracting networks

where networks with broader degree distribution are more robust. In real world, however, not all nodes in one network depend on all nodes in the other network, so it is of interest to study the robustness of two partially interdependent scale-free networks. Parshani *et al.* [31] generalized the above framework [30] to study partially interdependent networks. In Ref. [31], Parshani *et al.* studied the case of partial coupling where only a fraction  $q$  of nodes in each network are interdependent. Their results for two interdependent Erdos-Renyi (ER) [32,33] networks show that there exists a critical  $q_c$ , below which the system shows a second order percolation transition, while above  $q_c$  a first-order discontinuous percolation transition occurs. The evolution of such a change from first-order to second-order for SF networks when  $q$  changes remained unclear, because the behavior of interdependent SF networks is much more complex.

In this paper, we study the robustness of two partially interdependent scale-free (SF) networks under random attack. We assume that only a fraction  $q$  of nodes in each network are interdependent. We find that for SF networks there are three types of behaviors for different  $q$ . In addition to first-order transition for large  $q$  and second-order for small  $q$ , there is a mixed first-second-order transition in intermediate  $q$  values. Specifically, we find: (i) As the coupling strength between the two networks,  $q$ , reduces from 1 to 0, the giant component,  $P_\infty$ , of the interdependent networks shows three different types of transitions with  $p$ . For  $q_1 < q \leq 1$ , an abrupt collapse transition occurs. In the range  $q_2 < q < q_1$ , a hybrid transition, which combines both abrupt and continuous transitions, appears. For  $q < q_2$ , a continuous second-order transition appears. (ii) The threshold  $q_1$ , which separates the first-order and the hybrid transition, is equal to 1 for  $\lambda \leq 3$  and decreases with increasing  $\lambda$ . When  $q_2 < q < q_1$ , at the steady state of the cascading failures, there exists a  $p$  value,  $p_c^{\text{jump}}$ , at which the coupled SF networks will suffer a

substantial damage due to cascading failures but a very small nonzero mutual giant cluster  $P_\infty$  will survive. For  $p < p_c^{\text{jump}}$ ,  $P_\infty$  will continuously approach 0 at  $p = p_c = 0$  for  $\lambda \leq 3$  and at  $p = p_c > 0$  for  $\lambda > 3$ . Thus, the theoretical critical threshold  $p_c = 0$  for  $\lambda \leq 3$  for single networks [7] is expected to be valid also for strictly partially interdependent networks.

(iii) For  $q < q_2$ , the percolation transition becomes a regular second-order transition, where  $P_\infty$  continuously decreases to zero with decreasing  $p$ .

## II. CASCADING FAILURES

### A. Initial failure in one network

When the system contains interdependent networks, which are several networks fully or partially coupled with each other, the initial attack on first network can trigger a systematic cascade of failures between the networks [30]. This can be explained as follows: suppose we have a system of two interdependent networks  $A$  and  $B$ . When, at the initial attack, a fraction  $1 - p$  of nodes in network  $A$  ( $A -$  nodes) are removed since a fraction  $q$  of one-to-one bidirectional dependency links exists between  $A -$  nodes and  $B -$  nodes, so these  $B -$  nodes, which depend on the removed nodes in  $A$ , are also removed from the network  $B$ . Due to initial removal, network  $A$  may break into some connected parts, which are disconnected between themselves, called clusters. We assume that only the largest cluster (known as the giant component) will function and all the other smaller clusters will become dysfunctional. Then the malfunctioning of the nodes in the small clusters of network  $A$  will cause failures of their counterparts that depend on them in network  $B$ , so network  $B$  will also break into clusters and will cause further fragmentation in network  $A$ . This cascade of failures will keep going on iteratively until no further failures will occur.

To theoretically study the pair of coupled SF networks under random failures, we apply the framework developed by Parshani *et al.* [31] to study the cascading failures of partially interdependent random networks. Define  $p_A$  and  $p_B$  as the fraction of nodes belonging to the giant components of networks  $A$  and  $B$ , respectively. Define  $\psi'_n$  and  $\phi'_n$  as the fraction of network  $A$  nodes ( $A -$  nodes) and network  $B$  nodes ( $B -$  nodes) remaining, and  $\psi_n$  and  $\phi_n$  the giant components of networks  $A$  and  $B$ , respectively, after the cascade of failures stage  $n$ . Since  $\psi'_1$  stands for the remaining fraction of  $A -$  nodes after the initial removal, it follows that  $\psi'_1 = p$ . The remaining functional part of network  $A$  therefore contains a fraction  $\psi_1 = \psi'_1 p_A(\psi'_1)$ . Because a fraction  $q$  of nodes from network  $B$  depends on nodes from network  $A$ , the number of nodes in network  $B$ , which loses functionality, is  $(1 - \psi_1)q = q[1 - \psi'_1 p_A(\psi'_1)]$ . Similarly,  $\phi'_1 = 1 - q[1 - \psi'_1 p_A(\psi'_1)]$ , among these  $B -$  nodes, the fraction of nodes in the giant component of network  $B$  is  $\phi_1 = \phi'_1 p_B(\phi'_1)$ . The general form of the iterations is

$$\begin{aligned} \psi'_1 &= p, & \psi_1 &= \psi'_1 p_A(\psi'_1), \\ \phi'_1 &= 1 - q[1 - \psi'_1 p_A(\psi'_1)], & \phi_1 &= \phi'_1 p_B(\phi'_1), \\ \psi'_2 &= p\{1 - q[1 - p_B(\phi'_1)]\}, & \psi_2 &= \psi'_2 p_A(\psi'_2), \dots, \\ \psi'_n &= p\{1 - q[1 - p_B(\phi'_{n-1})]\}, & \psi_n &= \psi'_n p_A(\psi'_n), \\ \phi'_n &= 1 - q[1 - p_A(\psi'_n)p], & \phi_n &= \phi'_n p_B(\phi'_n). \end{aligned} \quad (1)$$

At the end stage of the cascade of failures when nodes failure stops, both networks reach a stable state where no further cascading failures happen. According to Eq. (1), it means

$$\phi'_m = \phi'_{m+1}, \quad \psi'_m = \psi'_{m+1}, \quad (2)$$

when  $m \rightarrow \infty$ , since eventually the clusters stop fragmenting.

Let  $\psi'_m$  be denoted by  $x$  and  $\phi'_m$  by  $y$ , so we get  $\psi_\infty = p_A(x)x$ ,  $\phi_\infty = p_B(y)y$ . Applying the previous conditions with the last two equations in Eq. (1), we obtain the set of equations

$$\begin{aligned} x &= p\{1 - q[1 - p_B(y)]\} \\ y &= 1 - q[1 - p_A(x)p]. \end{aligned} \quad (3)$$

Equation (3) [31] can be solved numerically to get the values of  $x$  and  $y$  when an analytical solution is not possible. This is the case for coupled SF networks, since the generating functions of SF network do not have a convergent analytical form, and only an infinite series can be obtained.

Next, we introduce the mathematical technique of generating functions for SF networks in order to get the analytical forms of  $p_A(x)$  and  $p_B(x)$  [30,31,35,36]. The generating function of the degree distribution is

$$G_A(z_A) = \sum_k P_A(k) z_A^k. \quad (4)$$

Analogously, the generating function of the underlying branching processes is

$$H_A(z_A) = G'_A(z_A)/G'_A(1). \quad (5)$$

Random removal of a fraction  $1 - p$  of nodes will change the degree distribution of the remaining nodes, so the generating function of the new distribution is equal to the generating function of the original distribution with the argument equal to  $1 - p(1 - z)$  [34,36]. The fraction of nodes in  $A$  that belongs to the giant component after the removal of  $1 - p$  nodes is

$$p_A(p) = 1 - G_A[1 - p(1 - f_A)], \quad (6)$$

where  $f_A$  is a function of  $p$ ,  $f_A \equiv f_A(p)$ , which satisfies the transcendental equation

$$f_A = G_A[1 - p(1 - f_A)]. \quad (7)$$

For SF networks, the degree distribution is  $P(k) = ck^{-\lambda}$ , where  $\lambda$  is the broadness of the distribution and  $k_{\min} < k < K$ . In the case of SF networks [4],

$$G_A(z_A) = \sum_{k=k_{\min}}^K \left[ \left( \frac{k_{\min}}{k} \right)^{\lambda-1} - \left( \frac{k_{\min}}{k+1} \right)^{\lambda-1} \right] z_A^k, \quad (8)$$

and

$$H_A(z) = \frac{\sum_{k=k_{\min}}^K k \left[ \left( \frac{k_{\min}}{k} \right)^{\lambda-1} - \left( \frac{k_{\min}}{k+1} \right)^{\lambda-1} \right] z_A^{k-1}}{\sum_{k=k_{\min}}^K k \left[ \left( \frac{k_{\min}}{k} \right)^{\lambda-1} - \left( \frac{k_{\min}}{k+1} \right)^{\lambda-1} \right]}. \quad (9)$$

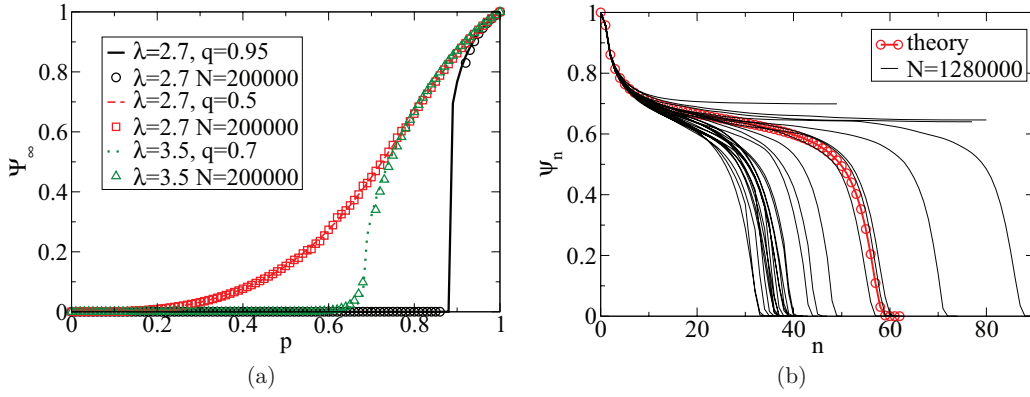


FIG. 1. (Color online) (a) The giant component  $\psi_\infty$  as a function of  $p$  for coupled SF-SF networks system under random removal of  $1 - p$  nodes in one network. SF networks with three different parameters are shown (i)  $\lambda = 2.7$ ,  $q = 0.95$ ,  $k_{\min} = 2$ ,  $\langle k \rangle = 3$  (solid black line and circles), (ii)  $\lambda = 2.7$ ,  $q = 0.5$ ,  $k_{\min} = 2$ ,  $\langle k \rangle = 3$  (dashed red line and squares), and (iii)  $\lambda = 3.5$ ,  $q = 0.7$ ,  $k_{\min} = 2$ , and  $\langle k \rangle = 3$  (dotted green line and triangles). The lines represent the theory [Eq. (3)] and symbols are results of simulations. (b) Comparison between theory and simulations of  $\psi_n$ , the fraction of the giant component obtained at  $p = 0.883$ , which is just below  $p_c$ , after  $n$  stages of the cascading failures for several random realizations of coupled SF networks with  $\lambda = 2.7$ ,  $k_{\min} = 2$ ,  $\langle k \rangle = 3$ ,  $q = 0.95$ , and  $N = 1280000$ . One can see that for the initial stages the agreement is perfect; however, for larger  $n$ , deviations occur due to random fluctuations in the topology between different realizations [37]. Both simulations and theoretical predictions show a plateau that drops to zero, corresponding to a complete fragmentation of the network. Note that some of the random realizations converge to a finite mutual giant component and are not completely fragmented.

From Eqs. (3)–(9), we obtain that

$$\begin{aligned}\phi_\infty &= \frac{(1 - z_A)[1 - G_A(z_A)]}{1 - H_A(z_A)}, \\ \psi_\infty &= \frac{(1 - z_B)[1 - G_B(z_B)]}{1 - H_B(z_B)},\end{aligned}\quad (10)$$

where  $z_A$  and  $z_B$  satisfy

$$\begin{aligned}\frac{(1 - z_B)}{1 - H_B(z_B)} &= 1 - q\{1 - p[1 - G_A(z_A)]\}, \\ \frac{(1 - z_A)}{1 - H_A(z_A)} &= p[1 - qG_B(z_B)].\end{aligned}\quad (11)$$

Substituting the generating functions of SF networks into the theoretical frameworks, Eqs. (1)–(7), we obtain, using numerical solutions, the theoretical results and compare them with results of computer simulations. Figure 1(a) shows good agreement between the theoretical and simulation results for the final giant component  $\psi_\infty$  as a function of  $p$  for two interdependent SF networks under random removal of  $1 - p$  nodes in one network. Three cases are studied: (i)  $\lambda = 2.7$ ,  $q = 0.95$ ,  $k_{\min} = 2$ ,  $\langle k \rangle = 3$ ; (ii)  $\lambda = 2.7$ ,  $q = 0.5$ ,  $k_{\min} = 2$ ,  $\langle k \rangle = 3$ ; and (iii)  $\lambda = 3.5$ ,  $q = 0.7$ ,  $k_{\min} = 2$ , and  $\langle k \rangle = 3$ . Figure 1(b) shows the cascading failure dynamics of the giant components left after  $n$  cascading stages (denoted by  $\psi_n$ ) as a function of number of iterations  $n$ , for several random realizations of SF networks, with  $\lambda = 2.7$ ,  $k_{\min} = 2$ ,  $\langle k \rangle = 3$  (same parameter values as the numerical calculation),  $N = 1280000$  at  $p = 0.883 < p_c$ , in comparison with the theoretical prediction of Eq. (1). Initially, the agreement is perfect, and when  $n$  is getting larger, the random fluctuations in topology of different realizations play an important role [37].

### B. Initial failures in both networks

When initially a  $1 - p$  fraction of nodes is removed from both networks [38,40], the system Eq. (3) becomes

$$\begin{aligned}x &= p\{1 - q[1 - p_B(y)p]\}, \\ y &= p\{1 - q[1 - p_A(x)p]\}.\end{aligned}\quad (12)$$

When the degree distribution of the two networks are the same, it follows that  $p_B(\cdot) = p_A(\cdot)$ ,  $x = y$ , and  $\phi_\infty = \psi_\infty$ , and the two Eqs. (12) become a single equation. Furthermore, using Eqs. (10) and (11), we obtain

$$\psi_\infty = \phi_\infty = \frac{(1 - z)[1 - G(z)]}{1 - H(z)},\quad (13)$$

where  $z$  satisfies

$$\frac{(1 - z)}{1 - H(z)} = p(1 - q\{1 - p[1 - G(z)]\}).\quad (14)$$

Equation (14) is a quadratic equation of  $q$ , and only one root has a physical meaning as

$$\frac{1}{p} = \frac{[H(z) - 1]\{1 - q + \sqrt{[(1 - q)^2 + 4q\phi_\infty(z)]}\}}{2(z - 1)} \equiv R(z).\quad (15)$$

The maximum of  $R(z)$  corresponds to  $p_c$ , and

$$p_c = \frac{1}{\max\{R(z_c)\}},\quad (16)$$

where  $z_c$  is obtained when  $z \rightarrow 1$ , i.e.,  $\phi_\infty = 0$ , and thus

$$\max\{R\} = \lim_{z \rightarrow 1} \frac{H(z) - 1}{z - 1}(1 - q) \doteq H'(1).\quad (17)$$

For two interdependent SF networks, when  $K \rightarrow \infty$ ,  $\max\{R\} \rightarrow \infty$ , so  $p_c = 0$ . However, in the numerical simulations,  $K$  cannot reach  $\infty$ , so  $p_c$  seems greater than 0, but in

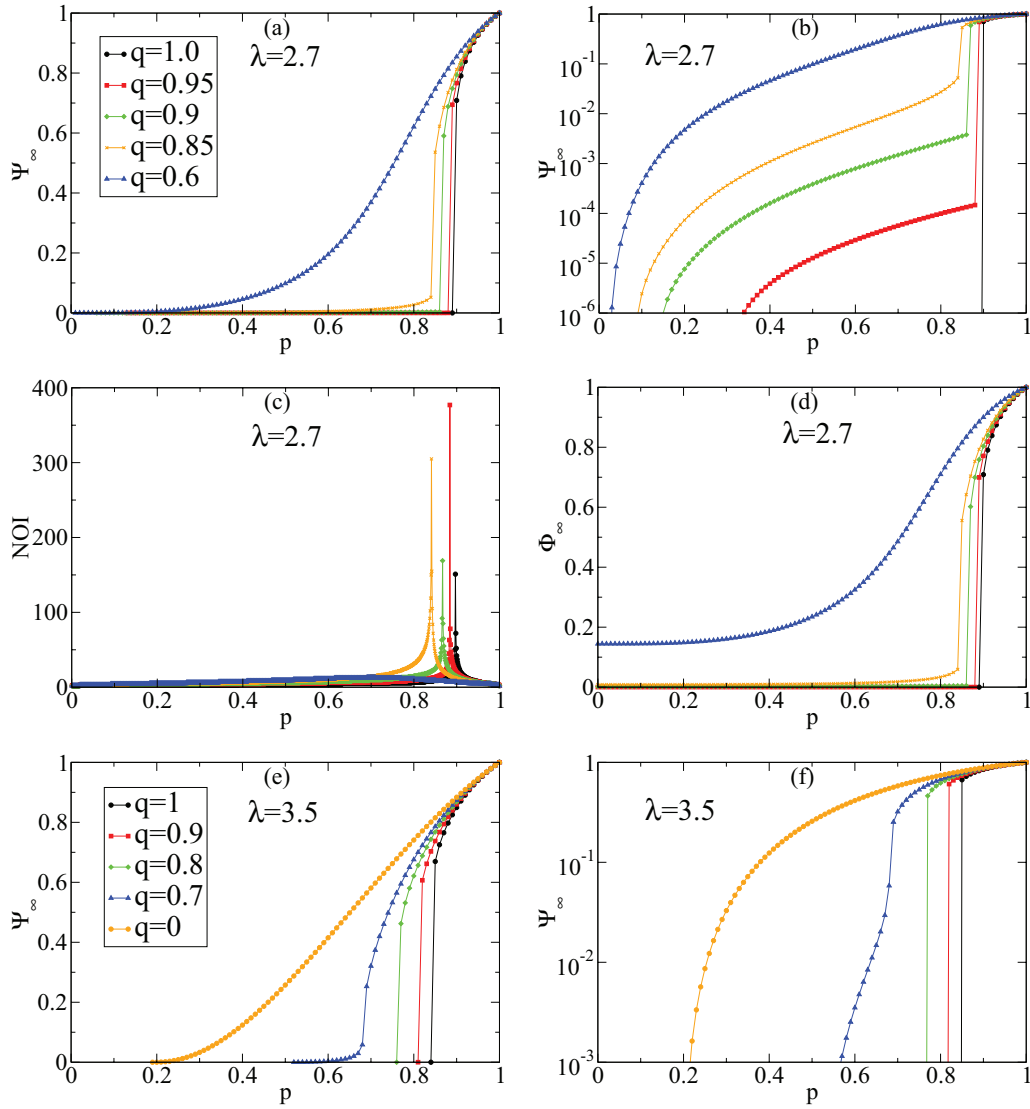


FIG. 2. (Color online) (a) and (b) Numerical calculations of coupled SF networks with  $\lambda = 2.7$ ,  $k_{\min} = 2$ , average degree  $\langle k \rangle = \langle k_A \rangle = \langle k_B \rangle = 3$ . The size of the giant mutually connected component,  $\psi_\infty$ , is shown as a function of  $p$  for several different values of  $q$  ( $q$  increases from left to right). Note that (b) is the same as (a) only that the y axis is in a logarithmic scale. We see that when  $q = 1$ , it is a first-order transition, since  $\psi_\infty$  goes to zero for  $p$  below the jump ( $p_c^{\text{jump}}$ ), but for  $q = 0.95$ ,  $q = 0.9$ , and  $q = 0.85$ , just below  $p_c^{\text{jump}}$ ,  $\psi_\infty$  first reaches a small *nonzero* value, then smoothly goes to zero at  $p = p_c = 0$  (For analytical proof, see Sec. II B). This is a typical property of hybrid phase transition. For  $q = 0.6$  there seems to be no jump of  $\psi_\infty$  and the transition is purely second-order. (c) The number of iterations (NOI) [43] to reach the end stage of cascade failure as a function of  $p$ . (d) Same plot as (a), but for  $\phi_\infty$ , which is the giant component of network B, which is not initially attacked. (e) and (f) are the same as (a) and (b) but for  $\lambda = 3.5$ , and for  $q = 1, 0.9, 0.8, 0.7$ , and  $0$ .

the theory  $p_c = 0$ . Note that when  $q = 1$ , Eq. (17) can yield for  $\max\{R\}$  a finite value since  $1 - q = 0$  and, therefore,  $p_c$  can become different from zero as found earlier.

Now let us relate  $p_c$  of failure in one network ( $p_c^o$ ) and both networks failures ( $p_c^b$ ). Our previous results [39] show that for two networks ( $p_c^o$ )<sup>2</sup> =  $p_c^b$ , so we argue that for two SF networks, when  $p_c^b = 0$ , it follows that  $p_c^o = 0$ .

### III. PERCOLATION BEHAVIOR

It is known that due to the existence of the interdependence links, when the two-network-system is under random attack, the iterative cascade of failures in both networks may result in

a percolation phase transition that completely fragments both networks when the initial fraction of removed nodes is above the critical threshold. When all nodes in both networks have one-on-one dependency links toward their counterpart nodes in the other network (given the size of both networks is the same), i.e.,  $q = 1$ , the percolation phase transition is discontinuous and first order [30]; and when the coupling strength  $q$  reduces to 0 (which becomes the case of a single SF network), a second-order percolation transition exists [7]. However, the change of transition from first- to second-order for SF networks when  $q$  changes remained unclear. For coupled ER [32,33] networks having Poissonian degree distribution, a critical point  $q_c$  exists. For  $q > q_c$ , a first-order transition occurs, while for  $q < q_c$ , a second-order continuous phase transition occurs [31].



The percolation behavior of two fully and partially interdependent SF networks, obtained from the numerical solutions of Eqs. (3)–(9), are shown in Fig. 2. Figures 2(a) and 2(b) show for  $\lambda = 2.7$ , the fraction of nodes in the giant component of network A,  $\psi_\infty$ , as a function of  $p$  (fraction of the initially unremoved nodes) for several  $q$  values. We can see, as expected, for SF networks, when  $q = 1$  (fully coupled), the phase transition is first-order [30]. This means as more and more nodes are initially removed, abruptly, at some value of  $p = p_c$ , the critical threshold, the iterative cascading failure process will completely fragment the system. Below  $p_c$ , there will not exist any cluster of the order of the network size. Thus, what still will remain are only very small clusters or single nodes. But just above this critical  $p$  value, when the failures stop, there exists a giant component in the system.

When  $q < 1$  but close to 1 ( $\lambda \leq 3$ ), as  $p$  decreases from 1,  $\psi_\infty$  first shows a sudden big drop similar to  $q = 1$  case, but  $\psi_\infty$  does not drop to 0, instead, it drops to a small but still *nonzero* value, which means though the giant cluster in the network suffers a big damage, it does not collapse completely [see Fig. 2(b)]. We name the  $p$  value where  $\psi_\infty$  has the discontinuous drop to be  $p_c^{\text{jump}}$ . We mathematically define the  $p_c^{\text{jump}}$  as

$$p_c^{\text{jump}} = \{p | \max[\psi_\infty(+p) - \psi_\infty(-p)]\}, \quad (18)$$

where  $+p$  denotes approaching  $p$  from above  $p$ , and  $-p$  denotes approaching  $p$  from below  $p$ .

As  $p$  keeps decreasing below  $p_c^{\text{jump}}$ , the small giant component,  $\psi_\infty$ , smoothly decreases, until at  $p = p_c = 0$ ,  $\psi_\infty$  will also reach 0. Thus, the real critical threshold for  $q < 1$  is  $p_c = 0$  similar to single networks [7] (see the analytical arguments at the end of Sec. II B). This phenomenon can be seen more clearly in Fig. 2(b), which is similar to Fig. 2(a) but the  $y$  axis,  $\psi_\infty$ , is plotted in a logarithmic scale. We see that at  $p_c^{\text{jump}}$ , for  $q = 0.95$ ,  $q = 0.9$ , and  $q = 0.85$ , the corresponding giant component sizes are reduced from order of 1 by a factor in the range of

$$\begin{aligned} \psi_\infty(-p_c^{\text{jump}}) &\in [10^{-2}, 10^{-4}], \\ \psi_\infty(+p_c^{\text{jump}}) &\approx o(1). \end{aligned} \quad (19)$$

When  $p$  decreases further,  $\psi_\infty$  decreases smoothly toward zero for  $p = 0$ . (The analytical proof is given in Sec. II B.)

This behavior is typical of the behavior of a hybrid transition, which includes both first- and second-order phase transition properties similar to that found in bootstrap percolation [41,42]. Note that our first-order transition is called hybrid transition by Baxter *et al.* [41], since the critical behavior above the transition is similar to second-order transition. The giant component first undergoes a sharp jump, which is a characteristic of first-order transition, and then smoothly goes to 0, which is a characteristic of a second-order phase transition. However, when  $q$  is getting smaller, this hybrid-transition phenomenon becomes less apparent, and the percolation phase behavior seems to become, at some threshold of  $q = q_2$ , an ordinary second-order transition. For example, the curve for  $q = 0.6$  in Figs. 2(a) and 2(b) seems to suggest a second-order transition, since there is no obvious sudden drop of the giant component size; instead, it continuously decreases when  $p$  decreases. For the case of two interdependent ER

networks, the system shows either a first-order or second-order phase transition but not a hybrid transition as here [30,38–40].

In network B, which is initially not attacked, similar behavior of the giant component  $\phi_\infty$  can be observed; see Fig. 2(d). However, the difference is that even at  $p = 0$ ,  $\phi_\infty$  does not approach 0 but reaches a finite value. This can be understood due to the partial dependency between the networks ( $q < 1$ ). Even if all nodes in A are removed ( $p = 0$ ), since  $q < 1$ , there is a finite fraction,  $1 - q$ , of nodes in B that are not removed, and in a SF network any finite fraction of unremoved nodes will yield a giant component [7]. Only in the fully coupled ( $q = 1$ ) case, the mutually connected giant cluster will completely collapse at  $p_c > 0$ .

#### A. Estimate of $p_c^{\text{jump}}$ from $P_\infty$ as a function of $p$

So far, we saw (Fig. 2) that for  $q_2 < q < q_1$ , as  $p$  decreases, the giant component shows an abrupt drop similar to a first order transition as Eq. (19). However, the drop is not to  $P_\infty = 0$ , like in a first-order transition, but to a small finite  $P_\infty$  value. As  $q$  decreases, as seen in Fig. 3, this drop becomes less sharp and smoother, and tends toward a continuous second-order transition as in Eq. (20). We analyzed this transition and find that the phase transition is like a first-order transition with a sharp drop of  $P_\infty$  at  $p_c^{\text{jump}}$ . For  $q < q_2$ , the hybrid transition diminishes and the behavior becomes a second-order transition with a continuous behavior. We are interested in determining the values of  $q_1$  and  $q_2$ , which separate the three distinct regions. In order to achieve that, we first need to find  $p_c^{\text{jump}}$ .

To accurately evaluate the values of  $p_c^{\text{jump}}$  for each  $q$ , we compute the number of iterations (NOI) in the cascading process, which shows a maximum at  $p_c^{\text{jump}}$  [43]. The NOI is the number of iterative cascade steps it takes the system to reach the equilibrium stage. In the simulations,  $\text{NOI} = m$  is defined by Eq. (2), i.e., the step where no further damage occurs. But in the numerical solution,  $\psi_n$  is approaching  $\psi_\infty$  only when  $n \rightarrow \infty$ . Here we define  $\text{NOI} = m$  when

$$\begin{aligned} \psi_m - \psi_{m+1} &< \xi, \\ \phi_m - \phi_{m+1} &< \xi, \end{aligned} \quad (20)$$

where  $\xi$  is a very small number. We choose  $\xi = 10^{-16}$  in this paper, which is equivalent to the requirement for the cascading failures to stop in a two-network system when both have  $10^{16}$  nodes. Note that for other very small values of  $\xi$ , the position of  $p_c^{\text{jump}}$  remains the same.

At the first-order and hybrid-order transition point, the NOI has its peak value, which drops sharply as the distance from the transition is increased [43]. Thus, plotting the NOI as a function of  $p$  provides a useful and precise method for identifying the transition point  $p_c^{\text{jump}}$  of the hybrid transition. Figure 2(c) presents such numerical calculation results of NOI. The transition point,  $p_c^{\text{jump}}$ , can be easily identified by the sharp peak characterizing the transition point. According to the NOI, we define  $p_c^{\text{jump}}$  as

$$p_c^{\text{jump}} = \{p | \max[\text{NOI}(p)]\}. \quad (21)$$

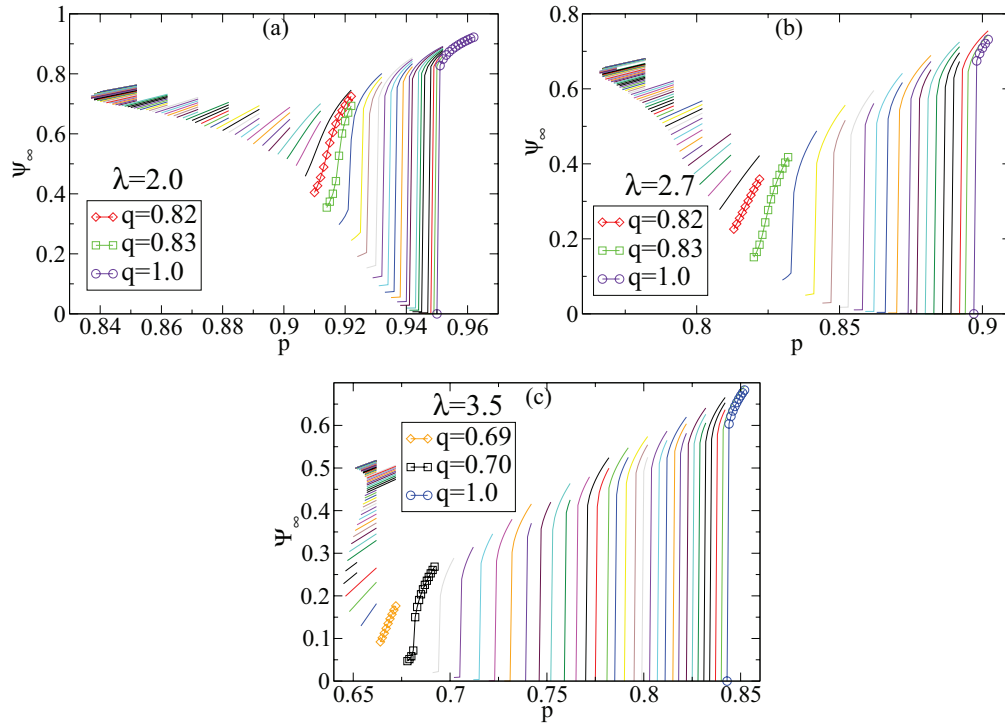


FIG. 3. (Color online) The giant component,  $\psi_\infty$  as a function of  $p$  for coupled SF networks with different values of  $\lambda$ , with  $k_{\min} = 2$ , and average degree  $\langle k \rangle = 3$ . Only the critical region around the maximum jump of  $\psi_\infty$  are shown, for different  $q$  values ranging from 0 (most left) to 1 (most right), with increments of  $q$  of 0.01. From these graphs, we can find as the  $q$  decreases,  $\psi_\infty$  becomes more continuous. It is also seen that for large  $q$  the sharp jump of  $\psi_\infty$  starts from small but *nonzero* values to large finite values. This behavior is typical to a hybrid-phase transition. (a)  $\lambda = 2.0$ , the threshold of hybrid transition and second-order transition is  $q_2 \cong 0.825$ , so the  $q = 0.82$  and  $q = 0.83$  curves are shown with symbols. We can see that the jump in  $\psi_\infty$  vanishes (shown by symbols) when  $q$  is reduced, as the phase transition becomes second-order. (b) For  $\lambda = 2.7$  and (c) for  $\lambda = 3.5$ , the curves in the region of  $q$  where the hybrid transition becomes second-order are shown by symbols.

From Fig. 2(c), one can see that the definition of Eq. (18) coincides with the definition of Eq. (21).

### B. Determining $q_2$

We know that when the transition is second-order, the order parameter  $\psi_\infty$  decreases continuously. As seen above,  $\psi_\infty$  has a maximum magnitude change at  $p_c^{\text{jump}}$ , which can be used to identify the position of  $p_c^{\text{jump}}$  by Eq. (21). Thus, we can now investigate these maximum magnitude changes for different  $q$  values at  $p_c^{\text{jump}}$ . In Fig. 3, we plot  $\psi_\infty$  as a function of  $p$  only near  $p_c^{\text{jump}}$ , for different  $q$  values ranging between 0 and 1, for several different  $\lambda$  values. In order to estimate when these changes are discrete and when they are continuous, we define

$$F(q) \equiv \log_{10} \left\{ \frac{\psi_\infty[+p_c^{\text{jump}}(q)]}{\psi_\infty[-p_c^{\text{jump}}(q)]} \right\}. \quad (22)$$

The rationale for this is as follows. The quantity  $\psi_\infty(+p_c^{\text{jump}})$  is the value of the order parameter just before the maximum drop at  $p > p_c^{\text{jump}}$ , and  $\psi_\infty(-p_c^{\text{jump}})$  is the value of the order parameter right after the maximum drop. In hybrid transition, as we discussed, this change in magnitude is large. However, as  $q$  becomes smaller, and when finally the transition becomes second-order, the change is continuous and the ratio between the magnitudes in Eq. (22) should become

1. Thus, whenever  $F(q)$  goes to 0, the corresponding  $q$  is  $q_2$ , which is the threshold where the hybrid transition turns into a second-order phase transition. When  $F(q) \rightarrow 0$ ,

$$\frac{\psi_\infty(+p) - \psi_\infty(-p)}{dp} \Big|_{p=p_c^{\text{jump}}} = 0. \quad (23)$$

By extrapolating these  $q$  positions [where  $F(q)$  goes to 0] for different  $\lambda$ , we get  $q_2$  as a function of  $\lambda$  and plot it in Fig. 4(a). Interestingly,  $q_2$  is not monotonic with  $\lambda$  but has a maximum around  $\lambda = 2.4$ . To alternatively identify  $q_2$ , we define the maximum slope as function of  $q$  as  $S(q)$ ,

$$S(q) \equiv \max \left\{ \frac{\psi_\infty(+p) - \psi_\infty(-p)}{dp} \Big|_{p=p_c^{\text{jump}}} \right\}. \quad (24)$$

When  $q$  is below or equal to  $q_2$ , the value of  $S(q)$  is very small, representing a continuous change of  $\psi_\infty$ , which is second-order; when  $q$  reaches some value, the  $S(q)$  has a sudden drop at  $q_2$ ; i.e., the maximum slope becomes dramatically large, representing a sharp change in  $\psi_\infty$ , which is a sign of the occurrence of a hybrid transition.

By identifying the position of  $q$  where the abrupt drop is located, we can also find the thresholds  $q_2$ , which distinguish second-order and hybrid transition. The results shown in Figs. 4(b)–4(d) match very well the results in Fig. 4(a), supporting our method for determining  $q_2$ .

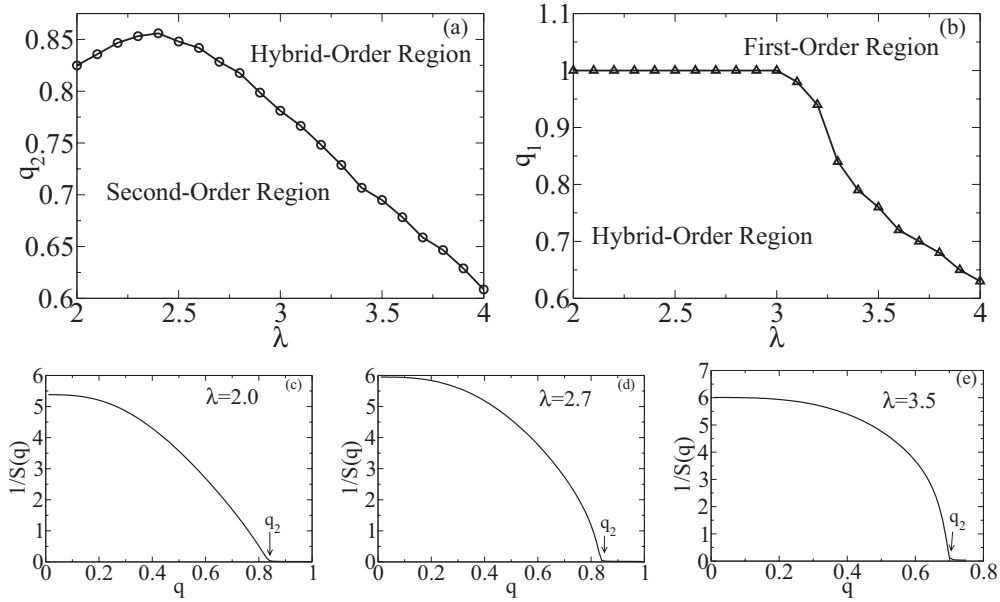


FIG. 4. (a) Values of  $q_2$  ( $\circ$ ) as a function of  $\lambda$  for SF networks with average degree  $\langle k \rangle = 3$  and  $k_{\min} = 2$ . Note the maximum of  $q_2$  at  $\lambda \cong 2.4$ . (b) Values of  $q_1$  ( $\triangle$ ) as a function of  $\lambda$ . Plot of  $1/S(q)$ , as a function of  $q$ , where  $S(q)$  is maximum slope value in the  $\psi$  vs.  $p$  plot, are shown for (c)  $\lambda = 2.0$ , (d)  $\lambda = 2.7$ , and (e)  $\lambda = 3.5$ , all SF networks are with average degree  $\langle k \rangle = 3$  and minimum degree  $k_{\min} = 2$ . We can see that the maximum slope values have a sharp change at  $q_2 = 0.83, 0.83$ , and  $0.7$  for  $\lambda = 2.0, 2.7$ , and  $3.5$ , respectively, supporting the results in (a).

### C. Determining $q_1$

For coupled SF networks with  $\lambda \leq 3$ , only when  $q = 1$  the transition is a first-order, which means  $q_1 = 1$  for  $\lambda \leq 3$ . As  $\lambda$  increases above 3,  $q_1$  becomes smaller than 1. To estimate the  $q_1$  values for  $\lambda > 3$ , we define according to Eq. (19) the system to have a first-order transition if  $\psi_\infty$  satisfies

$$\psi_\infty(p_c^{\text{jump}}, q) < \sigma. \quad (25)$$

Otherwise, it is not a first-order transition. We set here a value  $\sigma = 10^{-11}$ , but similar results have been obtained for  $\sigma = 10^{-12}$  and  $10^{-13}$ . We plot  $q_1$  as a function of  $\lambda$  obtained this way in Fig. 4(a).

Now, for any given  $\lambda$  value, we plot in Fig. 5,  $p_c$  as a function of  $q$  [ $p_c(q)$ ]. For  $\lambda \leq 3$ , only when  $q = 1$  it is a first-order transition, where  $\psi_\infty$  abruptly goes to 0 below  $p_c(1)$ ; when  $q < 1$ , it is either hybrid or second-order transition, and  $\psi_\infty$  is strictly 0 only at  $p = 0$  for both cases. However, since for the hybrid transition the giant component becomes very small at  $p_c^{\text{jump}}$ , we can regard this point as an effective  $p_c$ . For second-order transition, although there still exists a  $p$  value where there is a maximum change in the magnitude of  $\psi_\infty$ , but since  $\psi_\infty$  is continuous in all  $p$  region, we define  $p_c$  where  $\psi_\infty$  goes to 0 and, thus,  $p_c$  is always 0.

For  $\lambda > 3$ , the first-order transition happens also for  $q < 1$  and at  $p_c$ ,  $\psi_\infty$  jumps to 0. In this case,  $p_c$  of the second-order transition and of the hybrid transition is not 0.

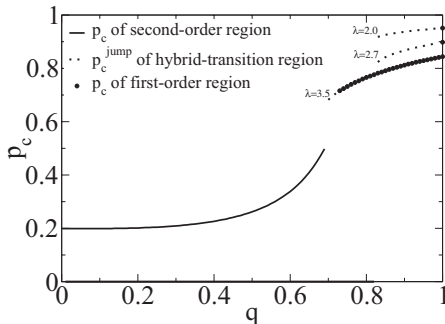


FIG. 5. The critical threshold  $p_c$  as a function of  $q$  for  $\lambda = 2.0, 2.7$ , and  $3.5$ . The values of  $p_c$  are defined as follows: for the first-order transition,  $p_c$  is where the  $\psi_\infty$  jumps to 0; for hybrid transition,  $p_c^{\text{jump}}$  is where the sudden jump of  $\psi_\infty$  to a nonzero  $\psi_\infty$  occurs; for second-order transition,  $p_c$  is where  $\psi_\infty$  goes to 0. For  $\lambda > 3$ , we can clearly see three regions of  $p_c$ . For  $\lambda < 3$ ,  $q_1 = 1$  and for  $q < q_2 \approx 0.83$ ,  $p_c^{\text{jump}}$  disappears and  $p_c$  becomes zero.

## IV. SUMMARY

We find that for two SF interdependent network models with partial dependency  $q$ , the phase transition behavior of the giant cluster under random attack shows a change from first-order (for  $q_1 < q < 1$ ), through hybrid transition ( $q_2 < q < q_1$ ), to a second-order phase transition ( $0 \leq q < q_2$ ). In the hybrid transition region, at an effective critical point  $p_c^{\text{jump}}$ , the giant component  $\psi_\infty$  has a sharp drop from finite value to a much smaller, yet a *nonzero* value. The hybrid transition seems to be unique for SF since it does not appear in coupled ER networks [31–33]. Our results demonstrate that SF coupled networks are more vulnerable (compared to ER) to random failures since  $p_c^{\text{jump}}$  is usually high and the breakdown leads to large drop of the size of the functional network. This is in agreement with Buldyrev *et al.* [30], showing that for broader degree distribution the coupled system is more vulnerable.

## ACKNOWLEDGMENTS

We thank DTRA and the Office of Naval Research for support. S.H. thanks the European LINC, EPIWORK, and

MULTIPLEX (EU-FET Project No. 317532) projects, the Deutsche Forschungsgemeinschaft (DFG), and the Israel Science Foundation for financial support.

- 
- [1] D. J. Watts and S. H. Strogatz, *Nature (London)* **393**, 440 (1998).  
 [2] A. L. Barabási and R. Albert, *Science* **286**, 509 (1999).  
 [3] M. E. J. Newman, *Networks: An Introduction* (Oxford University Press, New York, 2010).  
 [4] R. Cohen and S. Havlin, *Complex Networks: Structure, Robustness and Function* (Cambridge University Press, England, 2010).  
 [5] G. Caldarelli and A. Vespignani, *Large Scale Structure and Dynamics of Complex Webs* (World Scientific, Singapore, 2007).  
 [6] R. Albert and A. L. Barabási, *Rev. Mod. Phys.* **74**, 47 (2002).  
 [7] R. Cohen, K. Erez, D. ben-Avraham, and S. Havlin, *Phys. Rev. Lett.* **85**, 4626 (2000); **86**, 3682 (2001).  
 [8] D. S. Callaway, J. E. Hopcroft, J. M. Kleinberg, M. E. J. Newman, and S. H. Strogatz, *Phys. Rev. E* **64**, 041902 (2001).  
 [9] S. N. Dorogovtsev and J. F. F. Mendes, *Evolution of Networks: From Biological Nets to the Internet and WWW* (Oxford University Press, New York, 2003).  
 [10] C. Song, S. Havlin, and H. A. Makse, *Nature (London)* **433**, 392 (2005); *Nat. Phys.* **2**, 275 (2006).  
 [11] A. Bashan, R. Bartsch, J. Kantelhardt, S. Havlin, and P. Ivanov, *Nature Commun.* **3**, 702 (2012).  
 [12] A. Barrat, M. Barthelemy, and A. Vespignani, *Dynamical Processes on Complex Networks* (Cambridge University Press, England, 2008).  
 [13] T. P. Peixoto and S. Bornholdt, *Phys. Rev. Lett.* **109**, 118703 (2012).  
 [14] A. Zeng and W. Liu, *Phys. Rev. E* **85**, 066130 (2012).  
 [15] C. Schneider, A. Moreira, J. Andrade Jr., S. Havlin, and H. Herrmann, *Proc. Natl. Acad. Sci. USA* **108**, 10 (2010).  
 [16] S. Rinaldi, J. Peerenboom, and T. Kelly, *IEEE Control Systems Magazine*, vol. 21, no. 6 (2001), pp. 11–25.  
 [17] J. C. Laprie, K. Kanoun, and M. Kaaniche, *Lect. Notes Comput. Sci.* **54**, 4680 (2007).  
 [18] S. Panziera and R. Setola, *Int. J. Model. Ident. Contr.* **3**, 69 (2008).  
 [19] V. Rosato, L. Issacharoff, F. Tiriticco, S. Meloni, S. D. Porcellinis, and R. Setola, *Int. J. Crit. Infrastruct.* **4**, 63 (2008).  
 [20] A. Vespignani, *Nature (London)* **464**, 984 (2010).  
 [21] J. Goldenberg, Y. Shavitt, E. Shir, and S. Solomon, *Nature Phys.* **1**, 184 (2005).  
 [22] D. Zhou, H. E. Stanley, G. DiAgostino, and A. Scala, *Phys. Rev. E* **86**, 066103 (2012).  
 [23] R. G. Morris and M. Barthelemy, *Phys. Rev. Lett.* **109**, 128703 (2012).  
 [24] K. Zhao and G. Bianconi, arXiv:1210.7498 (2012).  
 [25] E. A. Leicht and R. M. D’Souza, arXiv:0907.0894 (2009).  
 [26] Z. Wang, A. Szolnoki, and M. Perc, *Scientific Reports* **3**, 1183 (2013).  
 [27] C. M. Schneider, N. A. M. Araujo, and H. J. Herrmann, arXiv:1301.2851 (2013).  
 [28] M. Pocock, D. Evans, and J. Memmott, *Science* **335**, 973 (2012).  
 [29] W. Cho, K. Goh, and I. Kim, arXiv:1010.4971 (2010).  
 [30] S. V. Buldyrev, R. Parshani, G. Paul, H. E. Stanley, and S. Havlin, *Nature (London)* **464**, 1025 (2010).  
 [31] R. Parshani, S. V. Buldyrev, and S. Havlin, *Phys. Rev. Lett.* **105**, 048701 (2010).  
 [32] P. Erdős and A. Rényi, *Publ. Math.* **6**, 290 (1959); *Publ. Math. Inst. Hung. Acad. Sci.* **5**, 17 (1960).  
 [33] B. Bollobás, *Random Graphs* (Academic, London, 1985).  
 [34] J. Shao, S. V. Buldyrev, L. A. Braunstein, S. Havlin, and H. E. Stanley, *Phys. Rev. E* **80**, 036105 (2009).  
 [35] J. Shao, S. V. Buldyrev, R. Cohen, M. Kitsak, S. Havlin, and H. E. Stanley, *Europhys. Lett.* **84**, 48004 (2008).  
 [36] M. E. J. Newman, *Phys. Rev. E* **66**, 016128 (2002).  
 [37] D. Zhou, A. Bashan, Y. Berezin, R. Cohen, and S. Havlin, arXiv:1211.2330 (2012).  
 [38] J. Gao, S. V. Buldyrev, S. Havlin, and H. E. Stanley, *Phys. Rev. Lett.* **107**, 195701 (2011).  
 [39] J. Gao, S. V. Buldyrev, S. Havlin, and H. E. Stanley, *Phys. Rev. E* **85**, 066134 (2012).  
 [40] J. Gao, S. V. Buldyrev, H. E. Stanley, and S. Havlin, *Nat. Phys.* **8**, 40 (2012).  
 [41] G. J. Baxter, S. N. Dorogovtsev, A. V. Goltsev, and J. F. F. Mendes, *Phys. Rev. E* **82**, 011103 (2010); *Phys. Rev. Lett* **109**, 248701 (2012).  
 [42] Y. Hu, B. Ksherim, R. Cohen, and S. Havlin, *Phys. Rev. E* **84**, 066116 (2011).  
 [43] R. Parshani, S. V. Buldyrev, and S. Havlin, *Proc. Natl. Acad. Sci. USA* **108**, 1007 (2011).